Research article

Fuzzy sliding mode control for trajectory tracking of an electric powered wheelchair

Mohammed Mecifi[1],*, Abdelmadjid Boumediene[1] and Djamila Boubekeur[2]

[1] Electrical Engineering Department, Faculty of Technology, University of Tlemcen, Tlemcen, Algeria
[2] Oran1 University, Oran, Algeria

* Correspondence: Email: mecifi_moh@yahoo.fr.

Abstract: Various controllers have been applied to control the dynamics of Electric Powered Wheelchair (EPW) for people whose walking are difficult or impossible, due to illness or disability. This paper deals with the nonlinear control of an electric wheelchair based on the hybridization between fuzzy logic and sliding mode control called Fuzzy Sliding Mode Control (FSMC). The EPW is powered by two Permanent Magnet Synchronous Motors (PMSM) due to some advantageous features, such as high efficiency, high torque to the current ratio, low noise and robustness. This research aims to present the dynamic modelling of both EPW motors with Lagrangian method in the first step, and the application of fuzzy sliding mode control in the second. This control technique was presented in order to consider the full dynamic model while alleviating the chattering phenomenon and to increase trajectory tracking performance of the EPW in the presence of disturbances. However, the reference trajectory used is that generated by the fifth-degree polynomial interpolation, which ensures a regular trajectory that is continuous in positions, velocities and accelerations. Finally, numerical simulations are presented to show the evolution of electrical and mechanical quantities in order to verify the effectiveness of the control strategy.

1. Introduction

More often, impaired mobility results in fewer opportunities for socializing, engaging in leisure pursuits and pursuing goals. Due to this, physically impaired people are at heightened risk of depression, anxiety, and social isolation. By providing an adapted aid to mobility, an electric powered wheelchair can significantly improve the quality of life of a physically disabled person [1,2].

The kinematic and dynamic modelling of electric powered wheelchair confirms its multivariate nonlinear nature [3]. It is an electromechanical system whose complete analysis calls together the main disciplines: mechanical, electrical, power electronics, automatic, computer science [4,5].

Several strategies have focused on the EPW's velocity and direction control as well as trajectory tracking using different kinds of motors, such as DC Motor, PMSM [6], brushless DC motors; e.g., adaptive controller, neural control techniques [7], robust controllers [8], sliding mode [9,10], backstepping [4], fuzzy logic [11,12], fuzzy sliding mode [13,14].

The main objective purpose of this paper is to use the Lagrangian method to model the electric powered wheelchair with permanents magnets synchronous motor as an actuator, due to some advantageous features, such as high efficiency, high torque to current ratio, low noise and robustness. After that, the application of the Fuzzy Sliding Mode Controller (FSMC), which combines the Sliding Mode Control algorithm (SMC) with a Fuzzy Logic Control scheme (FLC). It is well known that sliding mode control algorithm can give good transient performance and system robustness. However, these performances are obtained at the price of certain disadvantages: the appearance of the chattering phenomenon caused by the discontinuous part of the control which can have a harmful effect on the actuators [15,16]; the system is subjected at all times to a high control in order to ensure its convergence to the desired state and this is not desirable. Hence the need to incorporate a fuzzy controller in the sliding mode control in order to obtain a robust and smooth control [17,18]. This combination makes it possible to overcome the problems of the chattering of the sliding mode control and of deficit in tools for analyzing of the fuzzy logic control without forgetting the reduction in the number of fuzzy rules. Moreover, the salient advantages of each control strategy are kept during control action. For example, the fuzzy system is used to approximate unknown functions, while the sliding mode approach adds the possibility of establishing stable adaptation laws [19–21]. Therefore, as a type of robust controller with strong points, FSMC has been widely used in many application fields [22–25].

After the introduction section, the document is structured as follows: Section 2 covers the dynamic modelling with Lagrangian method for electric powered wheelchair. After that, fuzzy sliding mode control applied to the global system is proposed in section 3. Simulations and result analysis are carried out in section 4. Finally, the conclusions are drawn in section 5.

2. Dynamic modelling of the EPW based on PMSM actuators

The dynamic model of the electric wheelchair is essential for the controller design and simulation analysis, it is determined according to the Lagrange method considering the different forces that affect its movement.

Lagrange dynamics approach is a very powerful method for formulating the motion equations of mechanical systems. This method is used to systematically derive the equations of motion by

considering the kinetic and potential energies of the given system [10,26].

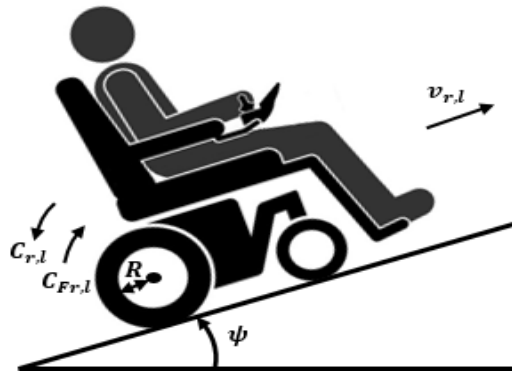To analyze the motion of this system; a fixed coordinate O-xy has been assigned as shown in Figure 1.

Figure 1. Wheelchair model for going up a slope.

Table 1 shows the meaning of the terms used in this paper.

The last two wheels are powered independently by two PMSM which their outputs are the right and left torque.

We start by establishing the equations of motion of the right and left motors, given by:

$$\begin{cases} J_a \frac{d\Omega_r}{dt} + f_v \Omega_r + C_r = C_{emr} \\ J_a \frac{d\Omega_l}{dt} + f_v \Omega_l + C_l = C_{eml} \end{cases} \tag{1}$$

Where:

$$C_{em} = P[(L_d - L_q)I_d I_q + \varphi_f I_q] \tag{2}$$

The nonlinear Park model of PMSM is defined in a rotor d-q reference frame by the following expression:

$$\begin{cases} \frac{dI_d}{dt} = -\frac{R_s}{L_d}I_d + P\Omega \frac{L_q}{L_d}I_q + \frac{1}{L_d}V_d \\ \frac{dI_q}{dt} = -P\Omega \frac{L_d}{L_q}I_d - \frac{R_s}{L_q}I_q - P\Omega \frac{\varphi_f}{L_q} + \frac{1}{L_q}V_q \end{cases} \tag{3}$$

The Lagrange equations of the right and left wheel can be written in the following form:

$$\begin{cases} \frac{d}{dt}\left(\frac{\partial L}{\partial \dot{\alpha}_r}\right) - \frac{\partial L}{\partial \alpha_r} = C_{Fr} - f_w \dot{\alpha}_r \\ \frac{d}{dt}\left(\frac{\partial L}{\partial \dot{\alpha}_l}\right) - \frac{\partial L}{\partial \alpha_l} = C_{Fl} - f_w \dot{\alpha}_l \end{cases} \tag{4}$$

Where $L = K - U$ is the Lagrangian function, K and U are the kinetic and potential energies of the system respectively.

Table 1. Parameters of the EPW.

Symbol	Description	Value
v	Longitudinal velocity of the EPW	m/s
α_r, α_l	Rotational angle of the right/left wheel	rad
α_{mr}, α_{ml}	Rotational angle of the right/left motor	rad
C_{emr}, C_{eml}	Electromagnetic torques of the right/left motor	$N.m$
C_{Fr}, C_{Fl}	Torque applied on the right/left wheel	$N.m$
C_r, C_l	Load torques required of the right/left motor	$N.m$
Ω_r, Ω_l	Angular rotor velocities of the right/left motor	rad/s
I_d, I_q	d- and q-axis stator currents	A
V_d, V_q	d- and q-axis stator voltages	V
M	EPW with operator mass	$210\ kg$
m_w	Mass of driving wheel	$2\ kg$
L	Distance between the two driving wheels	$0.57\ m$
l	Length of the EPW	$0.87\ m$
R	Radius of the driving wheel	$0.17\ m$
J	Moment of inertia of the EPW	$16.08\ kg.m^2$
J_w	Moment of inertia of the driving wheel	$0.0289\ kg.m^2$
g	Acceleration due to gravity	$9.81\ m/s^2$
ψ	Slope angle	$\%$
f_w	Viscous friction coefficient of the wheel	$0.008\ N.m.s/rad$
σ	Gear ratio	0.03
J_a	Moment of inertia of the motor	$0.0008\ kg.m^2$
f_v	Viscous friction coefficient of the motor	$0.00005\ N.m.s/rad$
R_s	Per phase stator resistance	$2.56\ \Omega$
L_d	d-axis stator inductances	$0.0064\ H$
L_q	q-axis stator inductances	$0.0056\ H$
φ_f	Permanent magnet flux	$0.06\ Wb$
P	Number of pairs of poles	4
P_n	Rated power	$400\ W$
N_n	Rated speed	$3000\ rpm$
V_n	Rated voltage	$120\ V$
I_n	Rated current	$2\ A$
Cem_n	Rated torque	$1.27\ N.m$

$$\begin{cases} \ddot{\alpha}_r \left(\left(m_w + \dfrac{M}{4} \right) R^2 + J_w + J \dfrac{R^2}{L^2} \right) + \ddot{\alpha}_l \left(\dfrac{M}{4} - \dfrac{J}{L^2} \right) R^2 + \left(m_w + \dfrac{M}{2} \right) gR\sin\psi = C_{Fr} - f_w \dot{\alpha}_r \\ \ddot{\alpha}_l \left(\left(m_w + \dfrac{M}{4} \right) R^2 + J_w + J \dfrac{R^2}{L^2} \right) + \ddot{\alpha}_r \left(\dfrac{M}{4} - \dfrac{J}{L^2} \right) R^2 + \left(m_w + \dfrac{M}{2} \right) gR\sin\psi = C_{Fl} - f_w \dot{\alpha}_l \end{cases} \tag{5}$$

Taking all these relations to introduce the motors dynamics in the total dynamic that includes the two-driver wheel as well as the total mass, the parameter which connects them is called gear reduction ratio noted by σ such as:

$$\begin{cases} \dot{\Omega}_r = \dfrac{1}{\sigma} \ddot{\alpha}_r \\ \dot{\Omega}_l = \dfrac{1}{\sigma} \ddot{\alpha}_l \end{cases} \tag{6}$$

$$\begin{cases} \Omega_r = \dfrac{1}{\sigma} \dot{\alpha}_r \\ \Omega_l = \dfrac{1}{\sigma} \dot{\alpha}_l \end{cases} \tag{7}$$

$$\begin{cases} C_r = \sigma C_{Fr} \\ C_l = \sigma C_{Fl} \end{cases} \tag{8}$$

The system has two degrees of freedom $[\alpha_r, \alpha_l]$, where their stored values are the displacements S_r and S_l such as:

$$\begin{cases} S_r = R\alpha_r \\ S_l = R\alpha_l \end{cases} \tag{9}$$

Then (1) becomes:

$$\begin{cases} \dfrac{1}{R} J_e \begin{pmatrix} \ddot{S}_r \\ \ddot{S}_l \end{pmatrix} + \dfrac{1}{R} C_e \begin{pmatrix} \dot{S}_r \\ \dot{S}_l \end{pmatrix} = \begin{pmatrix} C_{emr} \\ C_{eml} \end{pmatrix} + T \\ y = \begin{pmatrix} v \\ w \end{pmatrix} = \begin{bmatrix} R/2 & R/2 \\ -R/L & R/L \end{bmatrix} \begin{pmatrix} \dot{\alpha}_r \\ \dot{\alpha}_l \end{pmatrix} \end{cases} \tag{10}$$

Where $T = -\sigma \left(\dfrac{M}{2} + m_w \right) gR\sin\psi$, $J_e = \begin{bmatrix} a & b \\ b & a \end{bmatrix}$, $C_e = \begin{bmatrix} c & 0 \\ 0 & c \end{bmatrix}$.

With $a = \dfrac{J_a}{\sigma} + \sigma \left\{ J_w + \left(\dfrac{M}{4} + m_w \right) R^2 + \left(\dfrac{R}{L} \right)^2 J \right\}$, $b = \sigma R^2 \left(\dfrac{M}{4} - \dfrac{J}{L^2} \right)$, $c = \dfrac{1}{\sigma} f_v + \sigma f_w$.

Finally, the nonlinear global model of the EPW is as follow:

$$\begin{cases} \dot{x}_1 = x_2 \\ \dot{x}_2 = l_1 x_2 + l_2 x_4 + y_1 P\big[(L_d - L_q)x_5 x_7 + \varphi_f x_7\big] + y_2 p\big[(L_d - L_q)x_6 x_8 + \varphi_f x_8\big] + b_1 T \\ \dot{x}_3 = x_4 \\ \dot{x}_4 = l_3 x_2 + l_4 x_4 + y_3 P\big[(L_d - L_q)x_5 x_7 + \varphi_f x_7\big] + y_4 P\big[(L_d - L_q)x_6 x_8 + \varphi_f x_8\big] + b_2 T \\ \dot{x}_5 = -\dfrac{R_s}{L_d}x_5 + \dfrac{PL_q}{\sigma R L_d}x_2 x_7 + \dfrac{1}{L_d}V_{dr} \\ \dot{x}_6 = -\dfrac{R_s}{L_d}x_6 + \dfrac{PL_q}{\sigma R L_d}x_4 x_8 + \dfrac{1}{L_d}V_{dl} \\ \dot{x}_7 = -\dfrac{PL_d}{\sigma R L_q}x_2 x_5 - \dfrac{R_s}{L_q}x_7 - \dfrac{P\varphi_f}{\sigma R L_q}x_2 + \dfrac{1}{L_q}V_{qr} \\ \dot{x}_8 = -\dfrac{PL_d}{\sigma R L_q}x_4 x_6 - \dfrac{R_s}{L_q}x_8 - \dfrac{P\varphi_f}{\sigma R L_q}x_4 + \dfrac{1}{L_q}V_{ql} \end{cases} \quad (11)$$

Where $x = \big[S_r\ \dot{S}_r\ S_l\ \dot{S}_l\ I_{dr}\ I_{dl}\ I_{qr}\ I_{ql}\big]^T$, $B_v = [0\ b_1\ 0\ b_2]^T$, $u = \big[V_{dr}\ V_{dl} V_{qr}. V_{ql}\big]^T$, $V = T$.

With $l_1 = l_4 = -\dfrac{ac}{a^2-b^2}$, $l_2 = l_3 = \dfrac{bc}{a^2-b^2}$, $y_1 = y_4 = \dfrac{aR}{a^2-b^2}$, $y_2 = y_3 = -\dfrac{bR}{a^2-b^2}$, $b_1 = b_2 = \dfrac{R}{a+b}$.

The model obtained is multivariable (MIMO), nonlinear and strongly coupled.

Since both rear wheels are driven by two motors, the speed of each driving wheel is controlled independently. The electronic differential is therefore used to provide the required torque and speed references for each wheel. The slip on the rear wheels is ignored, so the speed of the wheels can be defined as a function of the radius of the wheels [27–29].
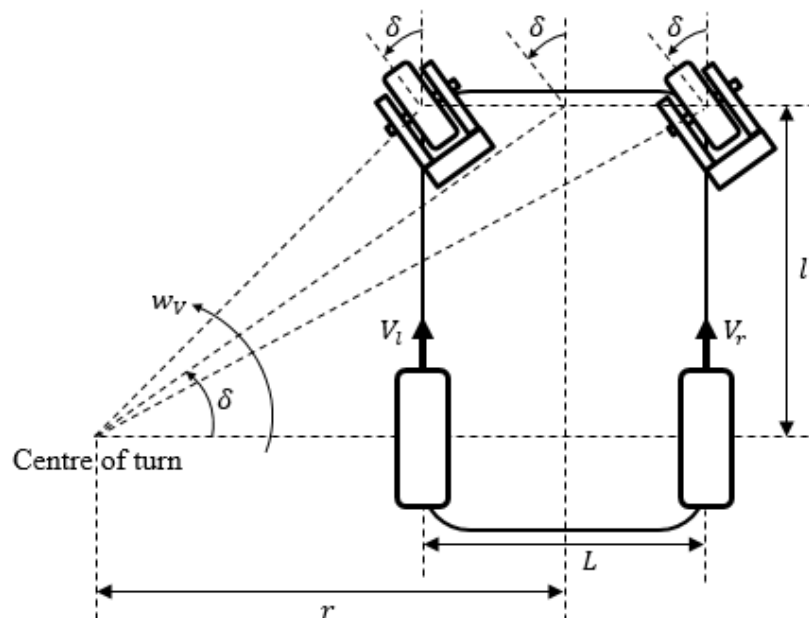
Figure 2 shows the steering left of the EPW.

Figure 2. EPW design model during steering.

The longitudinal speed of each wheel drive can be expressed as:

$$\begin{cases} V_l = w_V \left(r - \frac{L}{2} \right) \\ V_r = w_V \left(r + \frac{L}{2} \right) \end{cases}$$

(12)

Where $r = \frac{l}{tan\delta}$ and δ is the steering angle, the angular speeds are:

$$\begin{cases} w_l = \frac{l - \left(\frac{L}{2}\right)tan\delta}{l} w_V \\ w_r = \frac{l + \left(\frac{L}{2}\right)tan\delta}{l} w_V \end{cases}$$

(13)

If the steering angle $\delta > 0$, the EPW drives left and if $\delta < 0$, the EPW drives right. If $\delta = 0$, the EPW drives straight ahead (longitudinal movement).

w_V is the center angular speed, expressed by:

$$w_V = \frac{w_l + w_r}{2}$$

(14)

3. Fuzzy sliding mode control of the global system

The Sliding Mode Control is a very popular strategy for control of nonlinear uncertain systems, with a very large frame of applications fields. Due to the use of the discontinuous function, its main features are the robustness of closed-loop system and the finite-time convergence. Such technique consists on establishing a switching surface depending on existence and convergence laws, and then compels the dynamic behavior of the system to bring back toward this surface and slides around it till attaining the equilibrium state. This action is realized using a control law U as defined in (15) [30–32]. So, to tuning a sliding mode controller, requires to:

• Choose the sliding surface $S = 0$,
• Determine the existence and convergence conditions,
• Establish the appropriate control law which can be able to force the trajectory to match the manifold $S = 0$ and keep it switching around this surface.

$$U = U_{eq} + U_c$$

(15)

To find the sliding mode as given by (16), a general form that can be adopted [33]:

$$S(x) = \left(\frac{d}{dt} + \lambda \right)^{r-1} e(x)$$

(16)

Where $e(x)$ is the difference between the controlled variable and its reference, $\lambda \in \mathbb{R}_+^*$ and r is the relative degree of derivation number to be applied to the output signal x to generate explicitly the control component.

If S move towards 0, then e and its derivative are also lending to 0.

Concerning the convergence condition, it is recommended to define a scalar function which makes the surface $S = 0$ attractive and invariant. To do we can choose the Lyapunov function defined as:

$$V(x) = \frac{1}{2}S^2(x) \implies \dot{V}(x) = S(x)\dot{S}(x) \tag{17}$$

To insure the attractive phenomenon of the regulated variable toward the desired trajectory (reference), this function must realize:

$$\begin{cases} V(x) > 0 \\ \dot{V}(x) < 0 \end{cases} \tag{18}$$

In other words, we have [34]:

$$S(x)\dot{S}(x) < 0 \tag{19}$$

We will then analyze the behavior of our system controlled by sliding mode.

Let's put the error: $e = [e_r, e_l]^T = \left[S_r - S_{rref}, S_l - S_{lref}\right]^T$.

The model of the difference between the reference and the real trajectory, considering synchronous motors with non-salient poles ($L_d = L_q$), is:

$$\begin{pmatrix} \ddot{e}_r \\ \ddot{e}_l \end{pmatrix} = R \begin{bmatrix} a & b \\ b & a \end{bmatrix}^{-1} \left(\begin{pmatrix} V_{q_r} - R_s I_{q_r} - \frac{p\varphi_f}{\sigma R}\dot{S}_r - \frac{pL_d}{\sigma R}\dot{S}_r I_{d_r} \\ V_{q_l} - R_s I_{q_l} - \frac{p\varphi_f}{\sigma R}\dot{S}_l - \frac{pL_d}{\sigma R}\dot{S}_l I_{d_l} \end{pmatrix} - \frac{L_q}{Rp\varphi_f} \begin{bmatrix} c & 0 \\ 0 & c \end{bmatrix} \begin{pmatrix} \ddot{S}_r \\ \ddot{S}_l \end{pmatrix} \right) -$$
$$\begin{pmatrix} \ddot{S}_{rref} \\ \ddot{S}_{lref} \end{pmatrix} \tag{20}$$

Consider the following surfaces in the state space:

$$\begin{pmatrix} S_r \\ S_l \end{pmatrix} = \begin{pmatrix} k_1^2 e_r + 2k_1 \dot{e}_r + \ddot{e}_r \\ k_2^2 e_l + 2k_2 \dot{e}_l + \ddot{e}_l \end{pmatrix} \tag{21}$$

$$\begin{pmatrix} \dot{S}_r \\ \dot{S}_l \end{pmatrix} = \begin{pmatrix} k_1^2 \dot{e}_r + 2k_1 \ddot{e}_r + \dddot{e}_r \\ k_2^2 \dot{e}_l + 2k_2 \ddot{e}_l + \dddot{e}_l \end{pmatrix} \tag{22}$$

Replacing (20) in (22), we'll have:

$$\begin{pmatrix} \dot{S}_r \\ \dot{S}_2 \end{pmatrix} =$$

$$\frac{Rp\varphi_f}{L_q} \begin{bmatrix} a & b \\ b & a \end{bmatrix}^{-1} \left(\begin{pmatrix} V_{q_r} - R_s I_{q_r} - \frac{p\varphi_f}{\sigma R}\dot{S}_r - \frac{pL_d}{\sigma R}\dot{S}_r I_{d_r} \\ V_{q_l} - R_s I_{q_l} - \frac{p\varphi_f}{\sigma R}\dot{S}_l - \frac{pL_d}{\sigma R}\dot{S}_l I_{d_l} \end{pmatrix} - \frac{L_q}{Rp\varphi_f} \begin{bmatrix} c & 0 \\ 0 & c \end{bmatrix} \begin{pmatrix} \ddot{S}_r \\ \ddot{S}_l \end{pmatrix} \right) + \tag{23}$$

$$\begin{bmatrix} k_1^2 & 0 \\ 0 & k_2^2 \end{bmatrix} \begin{pmatrix} \dot{S}_r - \dot{S}_{rref} \\ \dot{S}_l - \dot{S}_{lref} \end{pmatrix} + \begin{bmatrix} 2k_1 & 0 \\ 0 & 2k_2 \end{bmatrix} \begin{pmatrix} \ddot{S}_r - \ddot{S}_{rref} \\ \ddot{S}_l - \ddot{S}_{lref} \end{pmatrix} - \begin{pmatrix} \dddot{S}_{rref} \\ \dddot{S}_{lref} \end{pmatrix}$$

So, the equivalent controls $V_{q_{r\_eq}}$ and $V_{q_{l\_eq}}$, which allow the sliding phenomenon to appear by bringing the state of the system back to the sliding surface defined by $\dot{S}_{r,l} = 0$, are calculated as follows:

$$\begin{pmatrix} V_{q_{req}} \\ V_{q_{leq}} \end{pmatrix} =$$

$$\frac{L_q}{Rp\varphi_f}\begin{bmatrix} a & b \\ b & a \end{bmatrix}\left(\begin{pmatrix} \ddot{S}_{rref} \\ \ddot{S}_{lref} \end{pmatrix} - \begin{bmatrix} k_1^2 & 0 \\ 0 & k_2^2 \end{bmatrix}\begin{pmatrix} S_r - S_{rref} \\ S_l - S_{lref} \end{pmatrix} - \begin{bmatrix} 2k_1 & 0 \\ 0 & 2k_2 \end{bmatrix}\begin{pmatrix} \dot{S}_r - \dot{S}_{rref} \\ \dot{S}_l - \dot{S}_{lref} \end{pmatrix}\right) +$$

$$\frac{L_q}{Rp\varphi_f}\begin{bmatrix} c & 0 \\ 0 & c \end{bmatrix}\begin{pmatrix} \ddot{S}_r \\ \ddot{S}_l \end{pmatrix} + \begin{pmatrix} R_s I_{q_r} \\ R_s I_{q_l} \end{pmatrix} + \begin{bmatrix} \frac{p\varphi_f + pL_d I_{d_r}}{\sigma R} & 0 \\ 0 & \frac{p\varphi_f pL_d I_{d_l}}{\sigma R} \end{bmatrix}\begin{pmatrix} \dot{S}_r \\ \dot{S}_l \end{pmatrix} \tag{24}$$

If the system states have not reached the sliding surfaces, the equivalent controls must be reinforced by another so-called robust control defined by:

$$\begin{pmatrix} V_{q_{r\_c}} \\ V_{q_{l\_c}} \end{pmatrix} = -\begin{pmatrix} U_1 sgn(S_r) \\ U_2 sgn(S_l) \end{pmatrix} \tag{25}$$

Where:

$$sgn(S) = \begin{cases} -1, & if\ S \leq 0 \\ 1, & if\ S > 0 \end{cases} \tag{26}$$

The global control is defined by:

$$\begin{pmatrix} V_{q_r} \\ V_{q_l} \end{pmatrix} = \begin{pmatrix} V_{q_{r\_eq}} + V_{q_{r\_c}} \\ V_{q_{l\_eq}} + V_{q_{l\_c}} \end{pmatrix} \tag{27}$$

By replacing (24) and (27) in (23) we find:

$$\begin{pmatrix} \dot{S}_r \\ \dot{S}_l \end{pmatrix} = \frac{Rp\varphi_f}{L_q}\begin{bmatrix} a & b \\ b & a \end{bmatrix}^{-1}\begin{pmatrix} V_{q_{r\_c}} \\ V_{q_{l\_c}} \end{pmatrix} \tag{28}$$

The attractiveness condition expressed by (19) becomes:

$$\begin{pmatrix} S_r\dot{S}_r \\ S_l\dot{S}_l \end{pmatrix} < 0 \Longrightarrow \left(\frac{Rp\varphi_f}{L_q}\begin{bmatrix} a & b \\ b & a \end{bmatrix}^{-1}\begin{pmatrix} S_r \\ S_l \end{pmatrix}\begin{pmatrix} V_{q_{r\_c}} \\ V_{q_{l\_c}} \end{pmatrix}\right) < 0 \tag{29}$$

In order to satisfy this condition, the sign of $\begin{pmatrix} V_{q_{r\_c}} \\ V_{q_{l\_c}} \end{pmatrix}$ must be opposite to that of $\frac{Rp\varphi_f}{L_q}\begin{bmatrix} a & b \\ b & a \end{bmatrix}^{-1}\begin{pmatrix} S_r \\ S_l \end{pmatrix}$.

The global control is finally given by:

$$\begin{pmatrix} V_{q_r} \\ V_{q_l} \end{pmatrix} =$$

$$\frac{L_q}{Rp\varphi_f}\begin{bmatrix} a & b \\ b & a \end{bmatrix}\left(\begin{pmatrix} \dddot{S}_{rref} \\ \dddot{S}_{lref} \end{pmatrix} - \begin{bmatrix} k_1^2 & 0 \\ 0 & k_2^2 \end{bmatrix}\begin{pmatrix} \dot{S}_r - \dot{S}_{rref} \\ \dot{S}_l - \dot{S}_{lref} \end{pmatrix} - \begin{bmatrix} 2k_1 & 0 \\ 0 & 2k_2 \end{bmatrix}\begin{pmatrix} \ddot{S}_r - \ddot{S}_{rref} \\ \ddot{S}_l - \ddot{S}_{lref} \end{pmatrix}\right) + \quad (30)$$

$$\frac{L_q}{Rp\varphi_f}\begin{bmatrix} c & 0 \\ 0 & c \end{bmatrix}\begin{pmatrix} \ddot{S}_r \\ \ddot{S}_l \end{pmatrix} + \begin{pmatrix} R_s I_{q_r} \\ R_s I_{q_l} \end{pmatrix} + \begin{bmatrix} \frac{p\varphi_f + pL_d I_{d_r}}{\sigma R} & 0 \\ 0 & \frac{p\varphi_f pL_d I_{d_l}}{\sigma R} \end{bmatrix}\begin{pmatrix} \dot{S}_r \\ \dot{S}_l \end{pmatrix} - \begin{pmatrix} U_1 sgn(S_r) \\ U_2 sgn(S_l) \end{pmatrix}$$

However, the main drawback of the sliding mode control is undesirable oscillations with finite amplitude and frequency due to the presence of unmodeled dynamics or discrete time implementation. This destructive phenomenon, so called "chattering", may lower control accuracy or incur unwanted wear of mechanical components.

Here, a hybridization methodology between fuzzy logic and sliding mode control is applied, the controller resulting from this combination is called "Fuzzy Sliding Mode Controller (FSMC)", This one presents the same structure of SMC, apart from the 2nd term U_c, which will be replaced by a fuzzy controller. For this, the term $-Usgn(S)$ can be replaced by a fuzzy controller. This controller has an input and an output, and the rule base is used to establish a connection between S and U_c. This is interpreted by rules of the form: $IF - THEN$ as shown in Table 2.

Table 2. Rule base of FLC.

IF	S	is	NB	THEN	U_c	is	VB (Very Big)
IF	S	is	NS	THEN	U_c	is	B (Big)
IF	S	is	Z	THEN	U_c	is	M (Medium)
IF	S	is	PS	THEN	U_c	is	S (Small)
IF	S	is	PB	THEN	U_c	is	VS (Very Small)

The fuzzy controller having an input S of five membership functions and an output U_c of five membership functions which are shown in Figure 3.
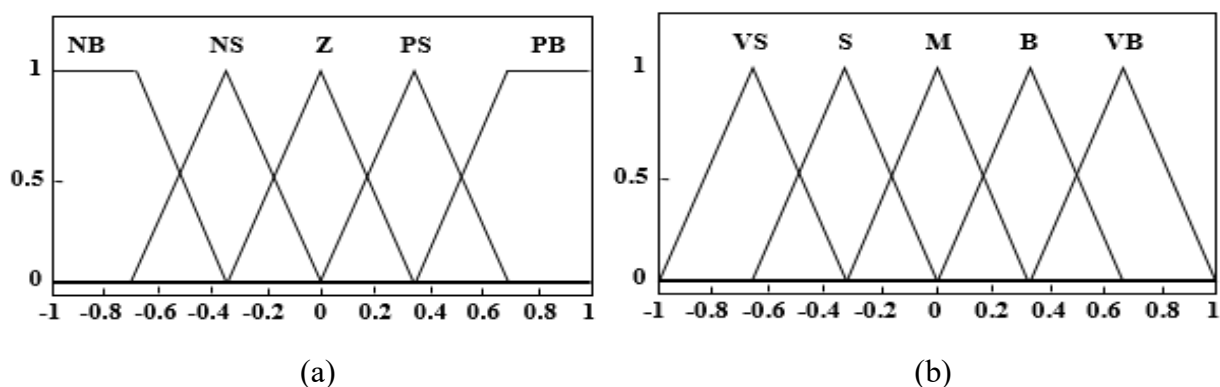

(a)   (b)

Figure 3. Membership functions of: (a) Input S_r, S_l, (b) Output $V_{q_{r\_c}}, V_{q_{l\_c}}$.

The second input of the system V_d is determined using the PMSM vector control to eliminate the nonlinearity of the system by maintaining the current I_d to zero and V_d takes its corresponding value as follow:

$$V_d = -p\Omega L_q I_q \tag{31}$$

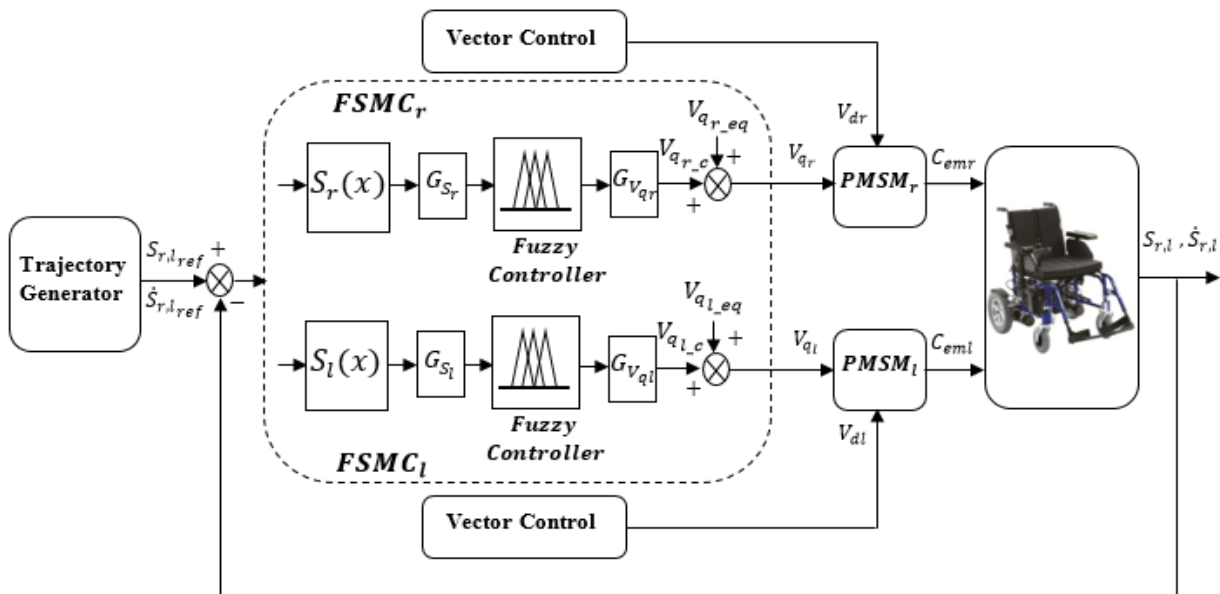Finally, the block diagram for the FSMC is illustrated in Figure 4.

Figure 4. Block diagram of the FSMC for the EPW control.

4. Simulation results and discussion

First, we start by generating the reference trajectory of the right and left wheel in order to assess the robustness of the trajectory tracking of the controller. The use of polynomial form (as set point) is a very practical tool for calculating trajectory.

The point-to-point trajectory between S^i and S^f is determined by the following equations:

$$S(t) = S^i + r(t)D \quad \text{for} \quad 0 \le t \le t_f \tag{32}$$

$$\dot{S}(t) = \dot{r}(t)D \tag{33}$$

With $D = S^f - S^i$; the boundary conditions of the interpolation function $r(t)$ are given by: $r(0) = 0$ and $r(t_f) = 1$.

Several interpolation functions can provide a trajectory, such as polynomial interpolation (linear interpolation, third degree polynomials (cubic) and fifth degree polynomials (quintic)), bang-bang acceleration profile and trapeze velocity profile [35]. The most frequently encountered polynomial interpolation method is the interpolation by the fifth degree polynomials, this method ensures a regular and continuous trajectory in displacements, velocities and accelerations.

To allow quintic to represent a complete trajectory, the trajectory needs to be separated into several phases (acceleration, steady state and deceleration). Each phase will be represented by a quintic equation [36,37]. To achieve the smooth transition from one phase to another, the boundary conditions for the initial and final position, velocity and acceleration must be satisfied.

The boundary conditions are as follows: $S(0) = S^i$, $S(t_f) = S^f$, $\dot{S}(0) = 0$, $\dot{S}(t_f) = 0$, $\ddot{S}(0) = 0$, $\ddot{S}(t_f) = 0$.

And, using the following polynomial form:

$$S(t) = a_0 + a_1 t + a_2 t^2 + a_3 t^3 + a_4 t^4 + a_5 t^5 \tag{34}$$

The expression (34) can also be written under the form (32) or (33) with the following interpolation function:

$$r(t) = 10 \left(\frac{t}{t_f}\right)^3 - 15 \left(\frac{t}{t_f}\right)^4 + 6 \left(\frac{t}{t_f}\right)^5 \tag{35}$$

For a displacement of $0\,m$ to $17.8\,m$ in $11.5\,s$ which correspond to a variable velocity up to $2.3\,m/s$, we have opted for the trajectories shown in Figure 5 by performing a slope variation from $\psi = 0\,\%$ to $\psi = 10\,\%$ in the time interval $t = 4.5\,s$ to $t = 5.5\,s$, and a direction change to the right from $\delta = 0\,°$ to $\delta = 0.1\,°$ between $t = 6\,s$ and $t = 7.5\,s$ achieved by the electronic differential. During this revolving, the wheels don't turn at the same velocity. Indeed, the left wheel travels more distance than the right wheel.
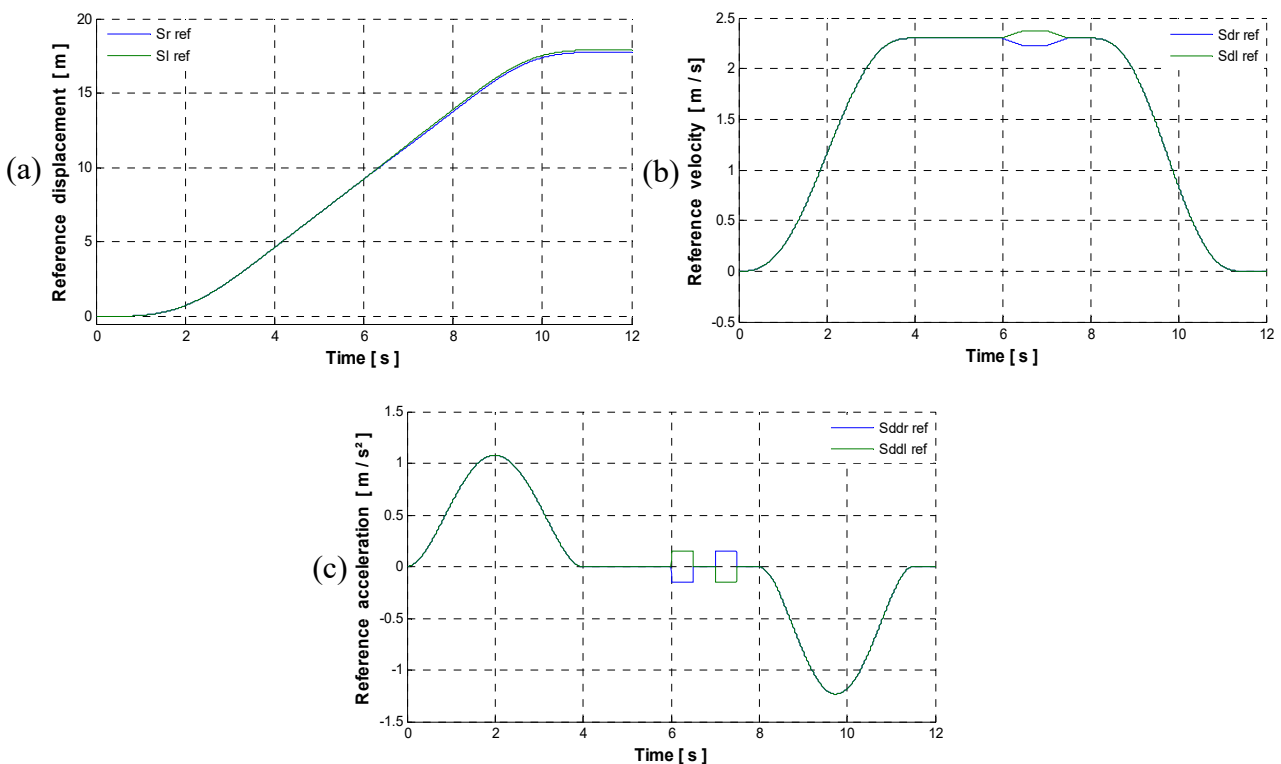

Figure 5. Reference trajectories of the right/left wheel: (a) Displacement, (b) Velocity, (c) Acceleration.

To evaluate the performance of the fuzzy sliding mode control applied to the EPW driven by two PMSMs with perfect voltage inverter, we simulate motion and velocity tracking in the presence of disturbances, we also show the evolution of electrical and mechanical quantities.

The consideration of this performance can be summarized in the following two cases:

4.1. Trajectory tracking

The Figure 6 and Figure 7 represent, respectively the displacement and velocity trajectory tracking of the right and left drive wheel, we note that the measured trajectories perfectly follow the references. This is verified by observing the tracking error curves $(S_{r,l_{ref}} - S_{r,l})$ and $(\dot{S}_{r,l_{ref}} - \dot{S}_{r,l})$, given in Figure 8 and Figure 9. The velocities increase to a maximum value which remains maintained during the steady state and then returns to zero, which corresponds to the final state.

Figure 10 shows the evolution of the electromagnetic torque $C_{emr,l}$ of the both PMSM, they increase to a maximum value, then they return to a very small positive value which remains constant in steady state, however, they react in case of slope variation, then they go to a negative minimum value and return to zero at the end. These torques are directly proportional to the stator quadrature currents $I_{qr,l}$ given in Figure 11. The stator direct currents $I_{dr,l}$ are maintained at zero by the vector control as shown in Figure 12. The direct and quadrature voltage inputs of both PMSM $(V_{dr,l}, V_{qr,l})$ and voltage feeding $(V_{ar,l})$ do not exceed their nominal values as shown in Figure 13, Figure 14 and Figure 15 respectively. Likewise, the turning and slope variation have no effect on all quantities of the system.

4.2. Robustness test

By performing for the same trajectory a variation of –50% of the global moment of inertia. The evolution of the electrical and mechanical quantities clearly shows the robustness of this control.

The results obtained show the efficiency and robustness of the Sliding Mode Controller of the global system (EPW+PMSM), with better tracking, fast response, without overshoot.
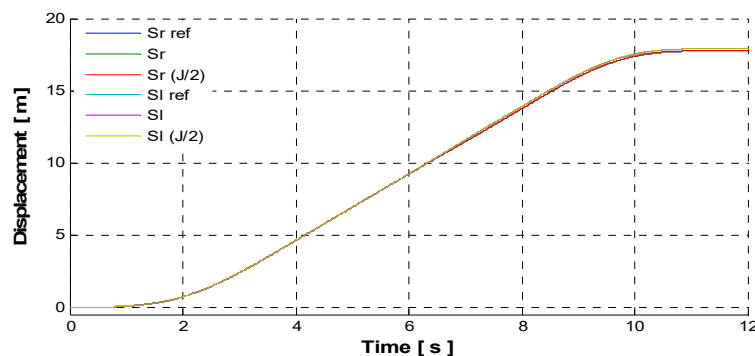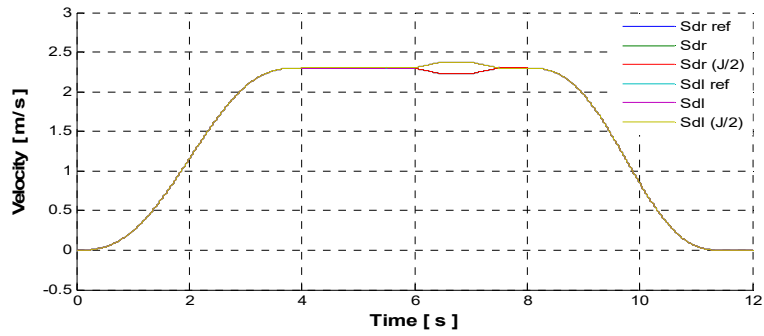

Figure 6. Displacement of the right/left wheel.

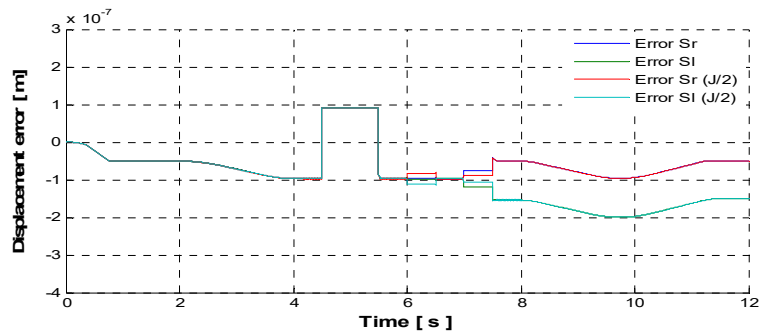**Figure 7.** Velocity of the right/left wheel.

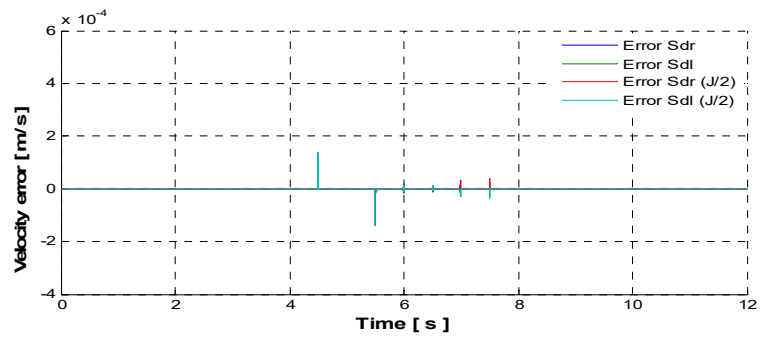**Figure 8.** Displacement error of the right/ left wheel.
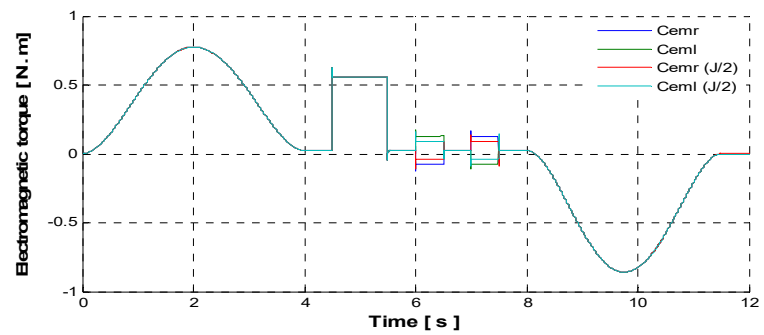

Figure 9. Velocity error of the right/ left wheel.

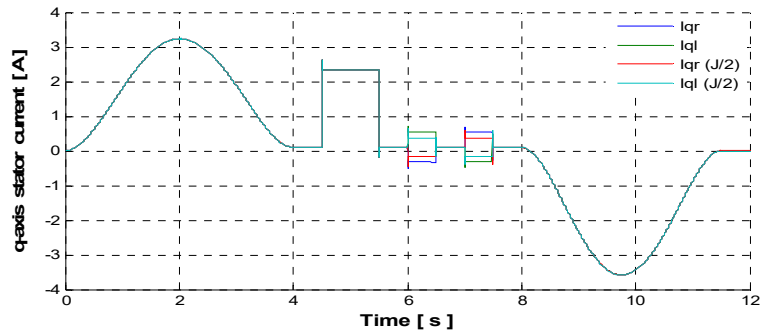**Figure 10.** Electromagnetic torque of the right/ left motor.
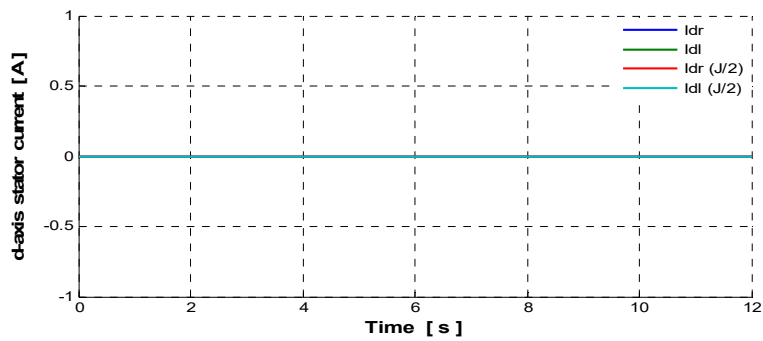
Figure 11. q-axis stator current of the right/left motor.

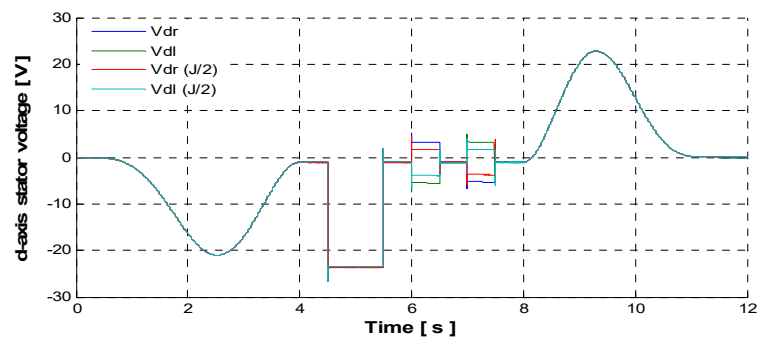**Figure 12.** d-axis stator current of the right/ left motor.

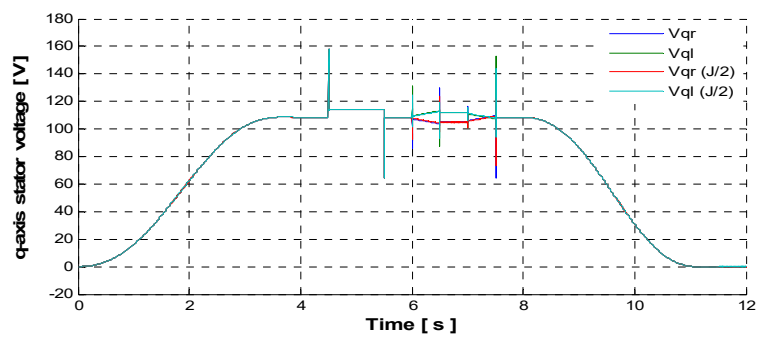**Figure 13.** d-axis stator voltage of the right/ left motor.

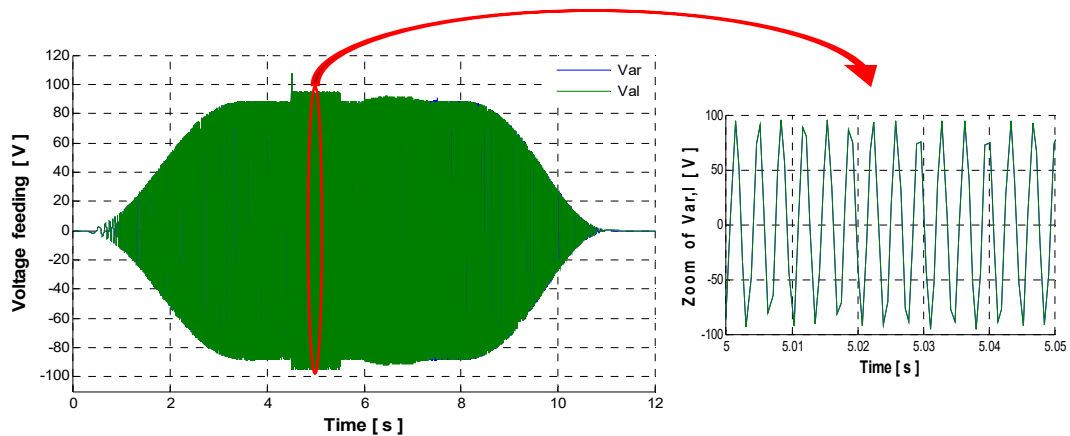**Figure 14.** q-axis stator voltage of the right/ left motor.

Figure 15. Voltage feeding of the right/ left motor.

5. Conclusions

In this study, a dynamic modelling of EPW using PMSM as an actuator according to the Lagrange method is considered. It is an electromechanical, multivariable, nonlinear and strongly coupled system, hence the necessity to introduce the robust controllers.

A nonlinear control by the fuzzy sliding mode controller was established to track the trajectory of the EPW. This technique based on the hybridization between fuzzy logic and sliding mode control provides a robust and smooth control with very satisfactory results for stabilization and precision.

The simulation results show the evolution of electrical and mechanical quantities, which are around their nominal values. These different results obtained confirm the feasibility of the fuzzy sliding mode controller of the global system (EPW+PMSM), with better tracking, fast response, without overshoot.

An experimental implementation of this controller is targeted in future work.

Conflict of interest

The authors declare that there is no conflict of interest in this paper.

References

1. Nguyen TN, Su SW, Nguyen HT (2011) Robust neuro-sliding mode multivariable control strategy for powered wheelchairs. *IEEE T Neur Sys Reh* 19: 105–111.
2. Al_Okby MFR, Neubert S, Stoll N, et al. (2017) Low-cost Hybrid Wheelchair Controller for Quadriplegias and Paralysis Patients. *Advances in Science Technology and Engineering Systems Journal* 2: 687–694.
3. Geonea I, Dumitru N, Dumitru V (2015) Design and Motion Analysis of a Powered Wheelchair. *Applied Mechanics and Materials* 772: 613–620.
4. Boubekeur D, Boumédiène A, Sari Z, et al. (2015) Modeling and Backstepping Control For Electric Powered Wheelchair. *International Electrical and Computer Engineering Conference*, Setif, Algeria.

5. Mecifi M, Boumédiène A, Boubekeur D (2019) A Fuzzy Logic Controller for Electric Powered Wheelchair Based on Lagrange Model. *International Conference on Advanced Electrical Engineering*, Algiers, Algeria.

6. Dou XX, Tong QM (2011) The Application of Permanent Magnet Electric Machine on Electrical Wheelchair. *Advanced Materials Research* 383: 7161–7165.

7. Boquete L, Garcia R, Berea R, et al. (1999) Neural control of the movements of a wheelchair. *Journal of Intelligent and Robotic Systems* 25: 213–226.

8. Ma J (2014) Design on Electric Power Wheel Control System. *Advanced Materials Research* 1070: 1668–1671.

9. Maatoug K, Njah M, Jallouli M (2019) Electric Wheelchair Trajectory Tracking Control based on Fuzzy Logic Controller. *19th International Conference on Sciences and Techniques of Automatic Control and Computer Engineering*, Sousse, Tunisia.

10. Kawasaki T, Yokoyama M, Tsuchiya M (2007) Sliding Mode Control for Electric Power Assist Systems. *Journal of System Design and Dynamics* 1: 159–167.

11. Ayten KK, Dumlu A, Kaleli A (2017) Real-Time Trajectory Tracking Control for Electric-Powered Wheelchairs Using Model-Based Multivariable Sliding Mode Control. *5th International Symposium on Electrical and Electronics Engineering*, Galati, Romania.

12. Bingül Z, Karahan O (2011) A Fuzzy Logic Controller tuned with PSO for 2 DOF robot trajectory control. *Expert Syst Appl* 38: 1017–1031.

13. Soltanpour MR, Khooban MH, Soltani M (2014) Robust fuzzy sliding mode control for tracking the robot manipulator in joint space and in presence of uncertainties. *Robotica* 32: 433–446.

14. Nafia N, El Kari A, Ayad H, et al. (2018) A robust type-2 fuzzy sliding mode controller for disturbed MIMO nonlinear systems with unknown dynamics. *Automatika* 59: 194–207.

15. Pang H, Yang J, Liang J, et al. (2018) On Enhanced Fuzzy Sliding-Mode Controller and Its Chattering Suppression for Vehicle Semi-Active Suspension System. *WCX World Congress Experience*, Detroit Michigan, United States.

16. Cao W, Lin C, Zhang L, et al. (2017) Fuzzy Sliding Mode Control of Networked Control Systems and Applications to Independent-Drive Electric Vehicles. *IEEE International Conference on Industrial Technology*, Toronto, Canada.

17. Yan TH, Wu B, He B, et al. (2016) A Novel Fuzzy Sliding-Mode Control for Discrete-Time Uncertain System. *Mathl Probl Eng* 2016: 1–9.

18. Bendaas I, Naceri F (2013) A New Method to Minimize the Chattering Phenomenon in Sliding Mode Control Based on Intelligent Control for Induction Motor Drives. *Serbian Journal of Electrical Engineering* 10: 231–246.

19. Zhang H, Fang H, Zhang D, et al. (2020) Adaptive Fuzzy Sliding Mode Control for a 3-DOF Parallel Manipulator with Parameters Uncertainties. *Complexity* 2020: 1–16.

20. Cherifi D, Miloud Y (2020) Hybrid Control Using Adaptive Fuzzy Sliding Mode Control of Doubly Fed Induction Generator for Wind Energy Conversion System. *Periodica Polytechnica Electrical Engineering and Computer Science* 64: 374–381.

21. Lei X, Jianqiao Z, Chuang L, et al. (2021) Fuzzy-logic-based adaptive event-triggered sliding mode control for spacecraft attitude tracking. *Aerosp Sci Technol* 108: 106394.

22. Song BK, An JH, Choi SB (2017) A New Fuzzy Sliding Mode Controller with a Disturbance Estimator for Robust Vibration Control of a Semi-Active Vehicle Suspension System. *Applied Sciences* 7: 1053.

23. Teng L, Bai S (2019) Fuzzy Sliding Mode Control of An Upper-Limb Exoskeleton Robot. *IEEE International Conference on Cybernetics and Intelligent Systems and IEEE Conference on Robotics, Automation and Mechatronics*, Bangkok, Thailand.

24. Soltanpour MR, Zaare S, Haghgoo M, et al. (2020) Free-Chattering Fuzzy Sliding Mode Control of Robot Manipulators with Joints Flexibility in Presence of Matched and Mismatched Uncertainties in Model Dynamic and Actuators. *J Intell Robot Syst* 100: 47–69.

25. Wang Y, Xie X, Chadli M, et al. (2020) Sliding Mode Control of Fuzzy Singularly Perturbed Descriptor Systems. *IEEE T Fuzzy Syst*, China.

26. Dhaouadi R, Abu Hatab A (2013) Dynamic Modelling of Differential-Drive Mobile Robots using Lagrange and Newton-Euler Methodologies: A Unified Framework. *Advances in Robotics and Automation* 2: 1–7.

27. Aggarwal A (2013) Electronic differential in electric vehicles. *International Journal of Scientific & Engineering Research* 4: 1322–1326.

28. Ozkop E, Altas IH, Okumus HI, et al. (2015) A fuzzy logic sliding mode controlled electronic differential for a direct wheel drive EV. *Int J Electron* 102: 1919–1942.

29. Tsai MC, Wu KS, Hsueh PW (2009) Synchronized Motion Control for Power-Wheelchairs. *Fourth International Conference on Innovative Computing, Information and Control*, Kaohsiung, Taiwan.

30. Sareena A, Mathew RP (2019) Application of PID Controller and Nonlinear Sliding Mode Control on Two Link Robotic. *International Journal of Engineering Research & Technology* 8: 504–508.

31. Ben Jridi A, Chaker N, Aloui H, et al. (2016) Sliding Mode Control for Speed's Tracking of an Electrical Vehicle. *Proceedings of the International Conference on Recent Advances in Electrical Systems*, Sfax, Tunisia.

32. Hosseini SH, Tabatabaei M (2017) IPMSM velocity and current control using MTPA based adaptive fractional order sliding mode controller. *Eng Sci Technol* 20: 896–908.

33. Irfan S, Mehmood A, Raeeaq MT, et al. (2018) Advanced sliding control techniques for inverted Pendulum: Modelling and simulation. *Eng Sci Technol* 21: 753–759.

34. Londhe PS, Patre BM (2019) Adaptive fuzzy sliding mode control for robust trajectory tracking control of an autonomous underwater vehicle. *Intel Serv Robot* 12: 87–102.

35. Dombre E, Khalil W (2007) Modeling, Performance Analysis and Control of Robot Manipulators. *ISTE,* London.

36. Qaid MM, Miskon MF, Bahar MB, et al. (2017) Comparative Study Between Quintic and Cubic Polynomial Equations Based Walking Trajectory of Exoskeleton System. *International Journal of Mechanical & Mechatronics Engineering* 17: 43–51.

37. Zhao X, Wang M, Liu N, et al. (2017) Trajectory Planning for 6-DOF Robotic Arm Based on Quintic Polynomial. *2nd International Conference on Control, Automation, and Artificial Intelligence*, Sanya, China.